Mechanical Systems and Signal Processing 200 (2023) 110511

Contents lists available at ScienceDirect

Mechanical Systems and Signal Processing

journal homepage: www.elsevier.com/locate/ymssp

A comprehensive methodology to obtain electrical analogues of linear mechanical systems

J. López-Martínez [a], D. García-Vallejo [b,*], A. Alcayde [a], S. Sánchez-Salinas [a], Francisco G. Montoya [a]

[a] Department of Engineering, University of Almería, Carretera de Sacramento s/n, 04120 Almería, Spain
[b] Department of Mechanical Engineering and Manufacturing, Universidad de Sevilla, Camino de los Descubrimientos s/n, 41092 Seville, Spain

ARTICLE INFO

Communicated by J. Rodellar

Keywords:
Full car model
Electric analogue
Electromechanical analogy
Vertical dynamics
3D 7-DOF car model analogue

ABSTRACT

Electrical analogues of linear mechanical systems have traditionally been obtained using a set of rules that can potentially be tedious when applied to complex systems. In addition, such rules do not cover all the possibilities of mechanical systems including rotational and translational generalized coordinates. The present work establishes a comprehensive and systematic methodology for obtaining the electrical analogue of any mechanical system modelled by rigid bodies, springs, and dampers. The method is simple and straightforward. First, the dynamic equations of the mechanical system are derived into matrix form. These equations are then translated to the electrical domain by means of the electromechanical analogy and, finally, the electrical circuit is obtained by direct inspection of the matrices. In addition, the method can deal with a combination of translational and rotational coordinates in the definition of the mechanical model. To support the proposed method, and beyond the planar vehicle models found in the literature, the electrical analogue of a linear 3D 7-DOF full car model is presented in this work.

1. Introduction

1.1. Motivation

The electromechanical analogy is an exceptionally versatile tool for the study and understanding of the combination of both mechanical and electrical systems. For example, it has been used since the 30–40 s of the twentieth century in the study of vibrations of linear mechanical systems from an electrical standpoint [1–5]. It consists of the study of electrical analogues of mechanical systems by using well-known methods for electrical networks. This paper aims to explore this analogy, in the context of linear models in vehicles and mechatronic systems. The proposed methodology is restricted to linear mechanical systems. Nevertheless, the literature shows a large number of works that utilizes electric analogues of linear mechanical systems. Therefore, the present method is expected to be useful for a significant number of researchers. Through the electromechanical analogy, this paper seeks to shed new light on how engineers can, for example, effectively design and operate efficient vehicle control systems and mechatronic structures using simple methods. Overall, this paper contributes toward the advancement of engineering knowledge by proposing a novel method to facilitate design strategies. Specifically, the new methodology proposed to obtain electrical analogues of linear mechanical systems is applied to a full car model. This is a representative example of a relatively complex problem that may

* Corresponding author.
E-mail addresses: javier.lopez@ual.es (J. López-Martínez), dgvallejo@us.es (D. García-Vallejo), aalcayde@ual.es (A. Alcayde), silvia.sanchez@ual.es (S. Sánchez-Salinas), pagilm@ual.es (F.G. Montoya).

https://doi.org/10.1016/j.ymssp.2023.110511
Received 12 January 2023; Received in revised form 25 April 2023; Accepted 6 June 2023
Available online 19 June 2023

Table 1
Classical analogy between variables in mechanical and electrical systems.

Mechanical variables			Electrical variables: Force-voltage			Force-current		
Force	[N]	F	u	Voltage	[V]	i	Current	[A]
Velocity	[ms^{-1}]	v	i	Current	[A]	u	Voltage	[V]
Stiffness	[Nm^{-1}]	k	S	Elastance	[F^{-1}]	B	Compliance	[H^{-1}]
Mass (inerter)	[kg]	m	L	Inductance	[H]	C	Capacitance	[F]
Damping	[Nsm^{-1}]	d	R	Resistance	[Ω]	G	Conductance	[Ω^{-1}]

be unaffordable using the known rules for obtaining electrical analogues of mechanical systems. Moreover, the topic of vehicle dynamics is one of the most discussed in the field of multibody system dynamics [6]. The results from this research will help the implementation of reliable solutions in several fields like electric mobility solutions across all industries. With this in mind, this paper is highly motivated by its potential to open up new horizons when exploring methods for improving vehicle performance using electromechanical analogies.

It is worth to note that this work does not pursue a gain in computational efficience but to offer mechatronic engineers a possibility to leverage well-established electrical analysis techniques in electrical analogues, leading to a more intuitive understanding and interpretation of the behaviour of the corresponding mechanical systems.

1.2. Background and literature review

In this section, the background on the electromechanical analogy is outlined along with a brief overview on the existing literature. In addition, a comparison with other techniques commonly found in the field is provided. An interesting reading about the beginnings and evolution of the electromechanical analogy is the work presented by Gardonio & Brennan [7]. More recently, the physical origins of the correspondences between the laws and the elements of the electrical, mechanical, and acoustic domains are discussed by Bertuccio [8].

Traditionally, two different approaches can be followed to obtain the electrical analogue of a mechanical system, i.e., the *force–voltage* and the *force–current* analogy. Historically, the force–voltage analogy (also known as *direct* analogy) was first introduced [2]. In this analogy, the force is related to the electrical voltage and the velocity to the current. Subsequently, the force–current analogy (also known as *inverse* analogy) was proposed as an alternative [1,9] to solve some issues encountered in the direct analogy. For example, the mechanical and electrical system preserves the same topology in the force–current analogy and may be more appropriate or easy to derive in some cases. The force–current analogy is also proposed in more recent studies as the best choice for robotics applications [10]. Nevertheless, both analogies are valid and can be applied to the same mechanical systems resulting in dual circuits [3]. Table 1 summarizes the relationships between variables and elements of mechanical and electrical systems for the force–voltage and force–current analogies. From the relations shown in this table, the electrical analogue of a mechanical system can be obtained by applying a set of rules, where the topology of both systems must maintain certain relationships [3,11,12]. However, these simple rules need to be further elaborated to analyse relatively complex mechanical systems, such as those presenting inertial coupling [13].

Beyond purely mechanical systems, the use of analogues is of notable interest in multidomain problems. For example, the case of an electrical rotating machine where the electrical subsystem is linked to the mechanical one. To deal with this kind of multidomain problems, the mechanical system is usually replaced with its electrical analogue and then attached to the existing electrical system [14,15]. The analogies between the different dynamic systems, such as mechanical, electrical, thermal, or fluid systems, are based on the similarity between their dynamic equations. Jeltsema and Scherpen [16] discuss the relationships between different physical domains on the basis of energy and power considerations. Recently, de Silva [17] proposed a systematic approach to unify multidomain systems into a single model with physically representative variables, including several illustrative examples.

The so-called electromechanical analogy is not the only approach to deal with multidomain dynamic systems. For example, *Bond Graph* (BG) graphical method has been frequently employed in the literature. In this method, the components of the system interact with each other through energy ports [18]. In addition, system components are combined by respecting their nature. Many authors have used the BG method to deal with mechatronic systems, see for instance [19–21]. Geitner [22] emphasizes BG as an excellent tool to study different abstraction levels and power flow structure comparison of dynamical systems. Sass et al. [23] compared three different modelling strategies (virtual work principle, linear graph and bond graph theories) to solve electromechanical multibody systems, concluding that BG is interesting for showing energy interactions between the different parts of the model. However, it has some limitations when considering complex three-dimensional (electro)mechanical systems. They pointed out several disadvantages, such as the difficulty of applying a causality assignment and the generation of constraints at the velocity level. Other authors have also pointed out the limitations of the BG method for complicated circuits, where the step-by-step procedure to achieve the BG scheme can become an issue [19]. In addition, once the graph for the system is obtained, the dynamical equations should be derived. This is not an easy task as highlighted in [23] due to its complexity, and therefore different simulation softwares are commonly used [19,22,24].

A remarkable utility of the analogy in multidomain systems is related to recent developments in vehicles in general, and electric vehicles in particular, such as in the modelling, optimization and control of vehicle suspension [25–30]. The electrical analogue

has also been used in the study of hybrid electric vehicle drive trains [31]. In these works, the electrical analogue of the vehicle suspension is used. Most authors adopt a 2-DOF model (quarter-car), while a more complex analogue model of a half-car is presented in [13]. However, the analogue of a complete model of the full car [32] has not been found in the literature. Such a model would be of interest in the design of active suspensions and control systems [33]. Another potential application related to automotive suspension systems is vibration energy harvesting in hydraulic shock absorbers [34–36], or in tyres, where the characteristic of piezoelectric materials is exploited to achieve an autonomous source of energy for sensors located inside the tyres [37–40].

In other fields, also focused on energy harvesting, electromechanical analogies have been used in applications including piezoelectric components [41–43], and in the analysis of electromechanical devices for the backpacks [44]. A significant number of works are related to the analysis of structural dynamic problems [45–48], as well as to the modelling of electromechanical systems [49–52] and Micro-Electro-Mechanical Systems (MEMS) [53]. Other interesting applications found in the literature include inductive power transfer systems [54], ultrasonic transducer arrays utilized in medical imaging and nondestructive testing applications [55], standing-wave linear ultrasonic motors models [56], and building an electrical circuit analog of a Hamiltonian system with non-holonomic constraint [57].

Therefore, the electromechanical analogy has proven useful in several fields, and it is expected that its use will be extended to new applications. The analogy between different physical domains has contributed to find new elements such as the inverter [58], or the memristor [59,60] and its mechanical analog, a tapered dashpot [61]. In addition, analogy is of interest in the educational field, where it is proposed as a tool that helps to understand different subjects [62].

1.3. Contributions

Typically, the electrical analogue of a mechanical system is obtained by applying a set of rules based on the relationships between variables and elements of mechanical and electrical systems [3,11]. However, as previously described, such rules can be tedious or even fail to provide a solution for complex systems, since they do not cover all possibilities. This is the case for mechanical systems presenting inertial coupling [13], or those that include rotational and translational generalized coordinates. Authors' previous work [13] dealt with obtaining the electrical analogue of two different 2D vehicle models, a half-car and a three-axle vehicle. To that aim, the known set of rules available in the scientific literature to generate an electric analogue by translating each mechanical element into the corresponding electrical one were applied. In addition, a new found analogy, not previously described, between inertial coupling and electrostatic capacitor coupling was presented there.

Unlike previously existing works, the present paper proposes a new methodology, based on the equivalence between the matrices of the mechanical equations and those of the electrical circuit analogue equations. This methodology allows to obtain analogues in a straightforward way, and facilitates the application of the approach to complex mechanical systems. To demonstrate the feasibility and broad applicability of the proposed methodology, we have presented an electrical analogue of a linear 3D 7-DOF full car model, which has not been previously published in the literature. The electrical analogue of such model is an example of a complex mechanical model in which the difficulty to obtain the electrical analogue by direct application of the usual rules on an element-by-element basis is evidenced. As will be shown, the present method can also handle a combination of translational and rotational coordinates in the definition of the mechanical model.

Overall, as a contribution and to facilitate the development and application of electro-mechanical analogy in complex systems, the present work establishes a comprehensive and systematic methodology to obtain the electrical circuit analogue of a mechanical system. Specifically, the aims of the present work are as follow:

(i) To establish a comprehensive and systematic methodology for obtaining the electrical analogue of any mechanical system modelled by rigid bodies, springs, and dampers.
(ii) To explain how the methodology can deal with a combination of translational and rotational coordinates in the definition of the mechanical model.
(iii) To develop the electrical analogue of a linear 3D 7-DOF full car model and to validate the electrical model through simulations.

1.4. Outline

The paper is organized as follows: Section 1 provides readers with background and context in the electromechanical analogy along with the contributions presented. Section 2 describes the methodology for obtaining electrical analogues of mechanical systems. A simple 2-DOF mechanical model is used as an example to better understand the process. In Section 3 the equation of motion of a 7-DOF full car model and its electrical analogue is derived and presented. The equivalence between both models is validated by simulations in Section 3.3. Section 5 discusses the salient features of the proposed method in comparison with other approaches, including previous research on the subject by the authors of this paper. Finally, Section 6 draws the main conclusions.

2. Comprehensive methodology to obtain electromechanical analogues

This section presents a comprehensive and systematic methodology to obtain electrical analogues of mechanical systems. The method applies to any linear multi-DOF model of a mechanical system modelled by rigid bodies, springs and dampers. The main advantages are its simplicity and systematic applicability. Inertial, damping and elastic couplings in the mechanical system are solved automatically without the need to interpret them as electrical couplings [13]. The key points of the method are explained in detail and illustrated using a simple example.

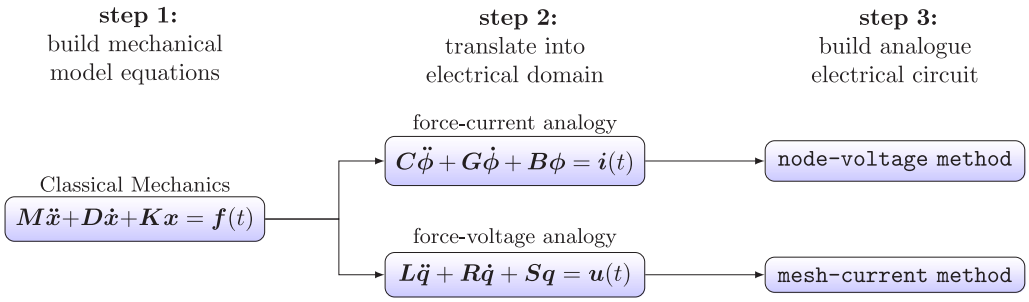

Fig. 1. Steps of the methodology.

2.1. Description of the method

An interesting feature of the proposed method is that it can be applied to any linear model of a mechanical system despite of the type of coordinates chosen, which can be either translational or rotational or a mixture of both types. The method presented here consists of three main steps as shown in Fig. 1 and is detailed as follows.

Step 1. Building the mechanical model equations

Firstly, the equations of motion are obtained for a given model of a mechanical system using any of the many methods of Classical Mechanics. The configurational state of a model with n degrees of freedom can be defined by means of a $n\times 1$ vector of generalized coordinates $\boldsymbol{x}$. When the generalized coordinate vector includes only one type of coordinates, either translational or rotational, it will be said that the coordinate vector is homogeneous. In the case that the set of coordinates includes both translational and rotational coordinates, a homogenization technique must be used to end up having an equivalent generalized coordinate vector containing only one type of coordinates, either rotational or translational, and therefore being homogeneous. The equations of motion can be expressed in the following matrix equation:

$$\boldsymbol{M}\ddot{\boldsymbol{x}}+\boldsymbol{D}\dot{\boldsymbol{x}}+\boldsymbol{K}\boldsymbol{x}=\boldsymbol{f} \tag{1}$$

where $\boldsymbol{M}$, $\boldsymbol{D}$ and $\boldsymbol{K}$ are $n\times n$ mass, damping, and stiffness matrices with constant elements, respectively. Variables $\ddot{\boldsymbol{x}}$, $\dot{\boldsymbol{x}}$ and $\boldsymbol{x}$ are the $n\times 1$ acceleration, velocity, and displacement time-dependent vectors, respectively, and $\boldsymbol{f}$ is the $n\times 1$ time-dependent force vector. Note that vectors are represented by bold and small letters, while matrices are represented by bold and capital letters. Non-bold letters represent scalars. Eq. (1) may be derived by using any of the existing methods to obtain the equations of motion of a mechanical system [63]. A systematic and commonly used method for systems with a large number of DOFs is Lagrange's method, see for example S.S. Rao [63]. In this work, Lagrange equations of the second kind in terms of the generalized coordinate vector $\boldsymbol{x}$ are expressed as

$$\frac{\mathrm{d}}{\mathrm{d}t}\left(\frac{\partial T}{\partial \dot{\boldsymbol{x}}}\right)-\frac{\partial T}{\partial \boldsymbol{x}}+\frac{\partial V}{\partial \boldsymbol{x}}+\frac{\partial F_R}{\partial \dot{\boldsymbol{x}}}=\boldsymbol{f}_a \tag{2}$$

where T and V are the kinetic and the potential energies, F_R is a Rayleigh dissipation function accounting for the energy dissipated by the dampers and $\boldsymbol{f}_a$ is the generalized applied force vector. Eq. (2) results in the equation of motion and can be expressed in the matrix form of Eq. (1). Note that $\boldsymbol{f}_a$ may be different from $\boldsymbol{f}$ of Eq. (1), since $\boldsymbol{f}$ may also include forcing terms arising from inertial, damping or stiffness forces as usually happens in systems with moving supports.

An important consideration in this first step is the need to use a vector with homogeneous coordinates, i.e., it can only contain rotational or translational coordinates but not a mixture of them. Otherwise, some equations would be formulated in terms of equilibria of forces and other equations would be formulated in terms of equilibria of moments, what precludes the direct application of the electrical analogy as described in this document. To overcome this issue, fictitious displacement/rotation coordinates can be defined instead of rotation/displacement coordinates. This approach results in obtaining a full set of homogeneous coordinates. An illustrative example of how to deal with mixed coordinates is shown in Section 2.2.2 below.

Step 2. Translation to the electrical domain

The second step of the method involves the translation of the differential equations to the electrical domain. This stage leads to a matrix system similar to the mechanical matrices shown in Eq. (1). The rationale is that the model dynamics are equivalent in both domains. Any of the two traditional approaches to obtain electrical analogues can be used, i.e. the *force–voltage* or the *force–current* analogy. Table 2 shows the equivalence between matrices and vectors of both domains. Note that this is consistent with the equivalence of variables in Table 1.

If the force–current analogy is used, then Eq. (1) for the mechanical system can be rewritten as

$$\boldsymbol{C}\ddot{\boldsymbol{\phi}}+\boldsymbol{G}\dot{\boldsymbol{\phi}}+\boldsymbol{B}\boldsymbol{\phi}=\boldsymbol{i} \tag{3}$$

Table 2
Analogue matrices and vectors for the mechanical and electrical domains.

Mechanical domain		Electrical domain			
		Force-voltage		Force-current	
Force	$\boldsymbol{f}$	$\boldsymbol{u}$	Voltage	$\boldsymbol{i}$	Current
Position	$\boldsymbol{x}$	$\boldsymbol{q}$	Charge	$\boldsymbol{\phi}$	Flux
Stiffness	$\boldsymbol{K}$	$\boldsymbol{S}$	Elastance	$\boldsymbol{B}$	Compliance
Mass	$\boldsymbol{M}$	$\boldsymbol{L}$	Inductance	$\boldsymbol{C}$	Capacitance
Damping	$\boldsymbol{D}$	$\boldsymbol{R}$	Resistance	$\boldsymbol{G}$	Conductance

where $\boldsymbol{C}$, $\boldsymbol{G}$ and $\boldsymbol{B}$ are the capacitance, conductance and compliance (inverse of inductance) matrices, respectively, $\boldsymbol{\phi}$ is the flux linkage vector ($\dot{\boldsymbol{\phi}} = \boldsymbol{u}$ is the node voltage vector) and $\boldsymbol{i}$ is the current source vector.

Similarly, by using the force–voltage analogy, Eq. (1) is rewritten as

$$\boldsymbol{L}\ddot{\boldsymbol{q}} + \boldsymbol{R}\dot{\boldsymbol{q}} + \boldsymbol{S}\boldsymbol{q} = \boldsymbol{u} \tag{4}$$

where $\boldsymbol{L}$, $\boldsymbol{R}$ and $\boldsymbol{S}$ are the inductance, resistance and elastance (inverse of capacitance) matrices, respectively, $\boldsymbol{q}$ is the charge vector ($\dot{\boldsymbol{q}} = \boldsymbol{i}$ is the current vector) and $\boldsymbol{u}$ is the voltage source vector.

It is worth noting that despite the clear preference in the literature for the force–current method over the force–voltage method (it better reflects the structure of the mechanical system) the methodology presented here is completely general. The choice of one method over the other is left to the researcher. It should be noted that the selection of one method or the other will result in a different (dual) circuit that can be solved by the most appropriate network analysis method.

Step 3. Building the electrical circuit analogue

The third step allows the electrical analogue circuit to be built by simple inspection of the matrices using the properties of the node-voltage method or the mesh-current method [64]. The usual way to proceed when using these methods is to obtain the matrices from existing electrical circuits. However, in the proposed methodology one proceeds oppositely, i.e. the electrical circuit is obtained from the matrices.

Both node-voltage and mesh-current methods are based on Kirchhoff's laws. They allow one to determine by simple inspection of the obtained matrices, whether an electrical element is connected between two nodes of a circuit and its value. The electrical circuits produced by the two approaches are dual to one another and hence reflect the same mechanical model in two distinct ways.

For the sake of brevity, the force–current analogy along with the node-voltage method will be used in the following sections. Thus, the application of the force–voltage analogy and mesh-current method is not presented in detail and is left to the reader. Those not familiar with these methods are referred to [64].

By means of the node-voltage method, the electric circuit can be built by inspection of the matrices in Eq. (3). The steps are enumerated as follows:

1. For a n-dimensional vector $\boldsymbol{u}$, a circuit diagram with $n+1$ nodes is built. The $n+1$ node is the reference or ground node (node 0) and is an analogue to the ground in a mechanical system.
2. For each entry a_{jk} in matrix $\boldsymbol{A} = \{\boldsymbol{C}, \boldsymbol{G}, \boldsymbol{B}\}$, the corresponding electrical elements are created between nodes following the rules below:
   (a) A non-zero off-diagonal ($j \neq k$) entry a_{jk} indicates an electrical element connected between node j and k. Note that all matrices are symmetric, and thus, $a_{jk} = a_{kj}$. The value of the element in the circuit is the matrix entry with an opposite sign.
   (b) An electrical element should be connected between node j and ground (0), if the sum of all off-diagonal elements in row j, $\sum a_{ji}$ with $i \neq j$, is not equal to the diagonal element a_{jj} (with opposite sign). The value of this electrical element is the sum of all elements in row j.
3. For every non-zero j entry in vector $\boldsymbol{i}$, a current source should be placed between node j and ground (0).

2.2. Application of the method

In the following, the 2-DOF mechanical model of Fig. 2 is used to illustrate the application of the proposed methodology in detail. The mechanical model consists of a bar of mass m and moment of inertia I_G, connected to the ground by two spring-damper pairs arranged in parallel and separated by a distance l. An external force $f(t)$ is acting on the centre of mass of the bar. For simplicity, the time dependence of the generalized applied force vector on time t will be omitted.

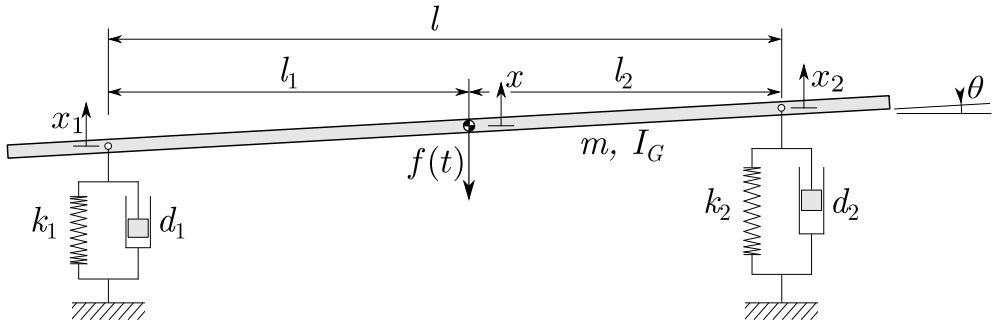

Fig. 2. 2-DOF mechanical model.

2.2.1. Using a homogeneous set of coordinates

As explained before, a homogeneous set of coordinates must only contain either translational or rotational coordinates, but not both types. In this example, the system can be modelled using two translational coordinates, therefore, using a homogeneous coordinate set. Let the displacements x_1 and x_2 be used as the independent variables, being the components of the generalized coordinates vector

$$\boldsymbol{x} = \begin{pmatrix} x_1 & x_2 \end{pmatrix}^T \tag{5}$$

The equations of motion can be obtained by using Lagrange equations shown in Eq. (2). The terms of kinetic energy L, potential energy V and Rayleigh dissipation function F_R can be written as follows:

$$\begin{aligned} T &= \frac{I_G\left(\dot{x}_1 - \dot{x}_2\right)^2}{2l^2} + \frac{m\left(l_1\dot{x}_2 + l_2\dot{x}_1\right)^2}{2l^2} \\ V &= \frac{k_1 {x_1}^2}{2} + \frac{k_2 {x_2}^2}{2} \\ F_R &= \frac{d_1\dot{x}_1^2}{2} + \frac{d_2\dot{x}_2^2}{2} \end{aligned} \tag{6}$$

The generalized force vector is obtained from the virtual work associated with the applied force, f. Then, the applied force, f, results in the following generalized force vector:

$$\boldsymbol{f}_a = \boldsymbol{f} = \begin{pmatrix} -\frac{f l_2}{l} \\ -\frac{f l_1}{l} \end{pmatrix} \tag{7}$$

Introducing T, V, F_R and $\boldsymbol{f}_a(t)$ into Eq. (2), the following ODE system is obtained:

$$\underbrace{\begin{pmatrix} \frac{{l_2}^2 m + I_G}{l^2} & \frac{l_1 l_2 m - I_G}{l^2} \\ \frac{l_1 l_2 m - I_G}{l^2} & \frac{{l_1}^2 m + I_G}{l^2} \end{pmatrix}}_{\boldsymbol{M}} \underbrace{\begin{pmatrix} \ddot{x}_1 \\ \ddot{x}_2 \end{pmatrix}}_{\ddot{\boldsymbol{x}}} + \underbrace{\begin{pmatrix} d_1 & 0 \\ 0 & d_2 \end{pmatrix}}_{\boldsymbol{D}} \underbrace{\begin{pmatrix} \dot{x}_1 \\ \dot{x}_2 \end{pmatrix}}_{\dot{\boldsymbol{x}}} + \underbrace{\begin{pmatrix} k_1 & 0 \\ 0 & k_2 \end{pmatrix}}_{\boldsymbol{K}} \underbrace{\begin{pmatrix} x_1 \\ x_2 \end{pmatrix}}_{\boldsymbol{x}} = \underbrace{\begin{pmatrix} -\frac{f l_2}{l} \\ -\frac{f l_1}{l} \end{pmatrix}}_{\boldsymbol{f}} \tag{8}$$

which may be written in the simple matrix form of Eq. (1).

Once the equations of motion of the mechanical system are obtained, vectors and matrices in Eq. (8) can be created using the force–current analogy as follows (see Table 2):

$$\begin{aligned} \boldsymbol{C} &= \boldsymbol{M} \\ \boldsymbol{G} &= \boldsymbol{D} \\ \boldsymbol{B} &= \boldsymbol{K} \\ \boldsymbol{\phi} &= \boldsymbol{x} \\ \boldsymbol{i} &= \boldsymbol{f} \end{aligned} \tag{9}$$

resulting in Eq. (3). Finally, following the rules of the node-voltage method, the circuit in Fig. 3(a) is obtained as a result of the force–current analogy in Fig. 2. The values of the electrical elements are:

$$C_1 = \frac{l_2 m}{l} \qquad G_1 = d_1 \qquad B_1 = k_1$$

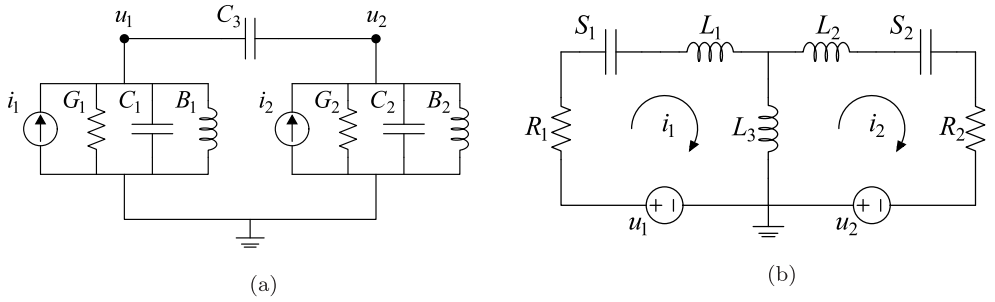

Fig. 3. (a) Force-current and (b) force–voltage analogues of the 2-DOF mechanical model of Fig. 2.

$$C_2 = \frac{l_1 m}{l} \qquad G_2 = d_2 \qquad B_2 = k_2$$

$$C_3 = \frac{I_G - l_1 l_2 m}{l^2} \qquad i_1 = -\frac{f l_2}{l} \qquad i_2 = -\frac{f l_1}{l}$$

As mentioned previously, a similar procedure could be carried out using the force–voltage analogy along with the mesh-current method, leading to the dual circuit shown in Fig. 3(b). For this dual circuit, the correspondence between the numerical values of the passive elements are $S_i \to B_i$, $L_i \to C_i$ and $R_i \to G_i$, while the sources are $u_i \to i_i$ and the mesh currents $i_i \to u_i$.

2.2.2. *Using a set of translational and rotational coordinates*

The electrical analogue of a mechanical system depends on the set of independent coordinates chosen. As shown in Fig. 2, the displacement of the centre of mass of the bar x, and the rotation angle θ, could also be selected as the independent variables. In such cases, the generalized coordinates of the vector include translational and rotational coordinates

$$\boldsymbol{x} = \begin{pmatrix} x & \theta \end{pmatrix}^T \tag{10}$$

To obtain a homogeneous coordinate vector, fictitious displacement coordinates can be defined instead of rotation coordinates. In this illustrative example, a fictitious displacement coordinate x_θ is defined as follows:

$$x_\theta = l\theta \tag{11}$$

which have a direct relation to angle θ. By introducing the new coordinate, x_θ, the full set of coordinates is now homogeneous and the generalized coordinate vector reads as

$$\boldsymbol{x} = \begin{pmatrix} x & x_\theta \end{pmatrix}^T \tag{12}$$

Note that distance l has been used as an arbitrary multiplying factor that allows having all equations written as force balances and all coordinates representing displacements. Thus, the force–current analogy can be directly applied. Interestingly, a different multiplying factor could be chosen without loss of generality. For instance, if a unit length is used, the value of angle θ can be read directly from the value of generalized coordinate x_θ.

Now, repeating the previously described procedure, the equations of motion obtained by using Lagrange equations result in

$$\underbrace{\begin{pmatrix} m & 0 \\ 0 & \frac{I_G}{l^2} \end{pmatrix}}_{\boldsymbol{M}} \underbrace{\begin{pmatrix} \ddot{x} \\ \ddot{x_\theta} \end{pmatrix}}_{\ddot{\boldsymbol{x}}} + \underbrace{\begin{pmatrix} d_1 + d_2 & \frac{l_2 d_2 - l_1 d_1}{l} \\ \frac{l_2 d_2 - l_1 d_1}{l} & \frac{{l_1}^2 d_1 + {l_2}^2 d_2}{l^2} \end{pmatrix}}_{\boldsymbol{D}} \underbrace{\begin{pmatrix} \dot{x} \\ \dot{x_\theta} \end{pmatrix}}_{\dot{\boldsymbol{x}}} + \underbrace{\begin{pmatrix} k_1 + k_2 & \frac{l_2 k_2 - l_1 k_1}{l} \\ \frac{l_2 k_2 - l_1 k_1}{l} & \frac{{l_1}^2 k_1 + {l_2}^2 k_2}{l^2} \end{pmatrix}}_{\boldsymbol{K}} \underbrace{\begin{pmatrix} x \\ x_\theta \end{pmatrix}}_{\boldsymbol{x}} = \underbrace{\begin{pmatrix} -f \\ 0 \end{pmatrix}}_{\boldsymbol{f}}. \tag{13}$$

The electrical analogue can be drawn by inspection of the matrices in Eq. (13) by using the node-voltage method. Fig. 4(a) shows the analogue result after applying the force–current to the mechanical system in Fig. 2. The values of the electrical elements are:

$$C_1 = m \qquad B_1 = \frac{l_2 k_1 + \left(l_1 + 2l_2\right) k_2}{l}$$

$$C_2 = \frac{I_G}{l^2} \qquad B_2 = \frac{\left(2{l_2}^2 + l_1 l_2\right) k_2 - l_1 l_2 k_1}{l^2}$$

$$G_1 = \frac{l_2 d_1 + \left(l_1 + 2l_2\right) d_2}{l} \qquad B_3 = \frac{l_1 k_1 - l_2 k_2}{l}$$

$$G_2 = \frac{\left(2{l_2}^2 + l_1 l_2\right) d_2 - l_1 l_2 d_1}{l^2} \qquad i_1 = -f$$

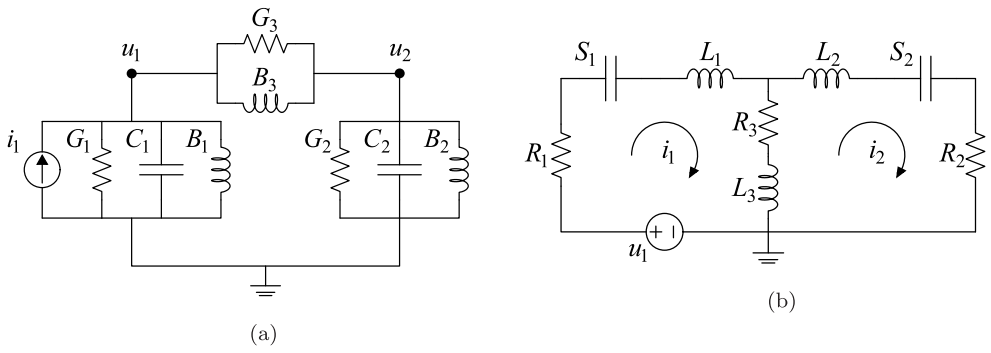

Fig. 4. (a) Force-current and (b) force–voltage analogues of the 2-DOF mechanical model of Fig. 2 with $\boldsymbol{x} = \begin{pmatrix} x & x_\theta \end{pmatrix}^T$.

$$G_3 = \frac{l_1 d_1 - l_2 d_2}{l}$$

Fig. 4(b) shows the result of the force–voltage analogy and the mesh-current method. For this circuit (dual of Fig. 4(a)), the values of the passive elements are $S_i = B_i$, $L_i = C_i$ and $R_i = G_i$, while the source is $u_1 = i_1$ and the mesh currents $i_i = u_i$.

It should be noted that Figs. 3 and 4 are both analogues of the same mechanical system shown in Fig. 2, but obtained using two different independent coordinate sets. It is interesting to note that using the first set of coordinates $\begin{pmatrix} x_1 & x_2 \end{pmatrix}$ the mass matrix is not diagonal, showing inertial coupling. On the contrary, using the second set of coordinates $\begin{pmatrix} x & \theta \end{pmatrix}$ the mass matrix is diagonal but the stiffness and damping matrix are not, showing elastic and damping coupling. With this second set of coordinates the force f, which is applied coincident with the variable x, is translated directly as a source with the same value.

3. Electric analogue of a linear 7-DOF full car model

In this section, the proposed methodology is applied to obtain the electrical analogue of a complex mechanical model such as the linear 7-DOF full car model. Based on the proposed methodology outlined in the previous section, the first step is to obtain the mechanical equations using any classical mechanical method available.

3.1. Mechanical model of the full car

The conceptualization of the full car model is presented in Fig. 5. It consists of the main frame that is allowed to translate vertically and rotate around the longitudinal axis (roll) and around a transversal axis (pitch). The motion of the main frame can be therefore described by three coordinates: the displacement of the centre of mass, x, the roll angle, α, and the pitch angle, β. Additionally, the displacement of three non-aligned points can be used to describe the vertical motion of the main frame. In this case, the centre of mass, the rear left and rear right attachment points can be selected. The main frame is supported by four similar sets of springs, dampers and masses representing the stiffness and damping properties of the suspensions and the tires along with the unsprung masses. In addition, the vertical displacements y_{di}, y_{dd}, y_{ti} and y_{td} of the left front, right front, left rear and right rear wheels, respectively, will be considered due to the uneven profile of the ground.

It should be noted that two different sets of coordinates can be used: a set that only includes translational coordinates or a set with a mixture of translational and rotational coordinates. Both sets of coordinates are widely used in the literature and deserve special consideration. Interestingly, they lead to different analogue electrical circuits.

3.1.1. Using only translational coordinates

According to the previous description, the number of degrees of freedom of the model is seven and the vector of generalized coordinates of the model, $\boldsymbol{x}$, using only translational coordinates, reads as follows

$$\boldsymbol{x} = \begin{pmatrix} x & x_{bi} & x_{bd} & x_{di} & x_{dd} & x_{ti} & x_{td} \end{pmatrix}^T \tag{14}$$

Using Lagrange equations in Eq. (2), the system's equations of motion have the following matrix structure:

$$\boldsymbol{M}\ddot{\boldsymbol{x}} + \boldsymbol{D}\dot{\boldsymbol{x}} + \boldsymbol{K}\boldsymbol{x} = \boldsymbol{f}_g + \boldsymbol{f}_y \tag{15}$$

where $\boldsymbol{f}_g$ is a 7×1 constant vector accounting for gravitational forces and $\boldsymbol{f}_y$ is a 7×1 time-dependent vector accounting for the dynamical loads induced by the unevenness of the ground.

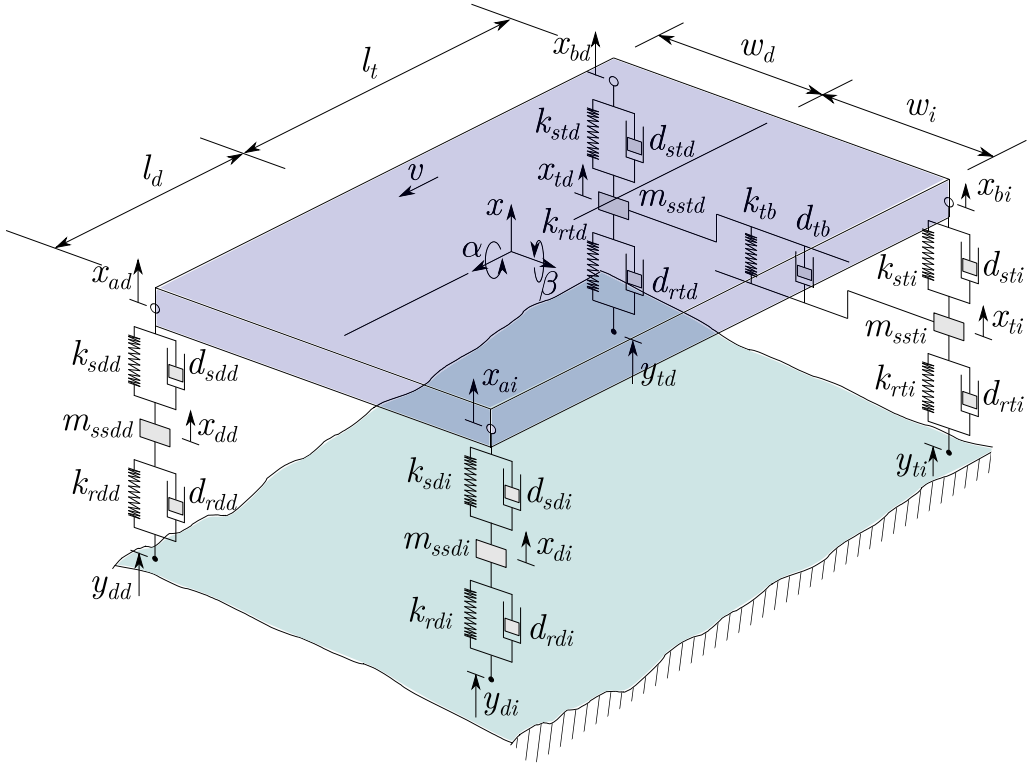

Fig. 5. 7-DOF model of the full car.

The mass matrix is symmetric and reads as follows:

$$\boldsymbol{M} = \begin{pmatrix} m_{11} & m_{12} & m_{13} & 0 & 0 & 0 & 0 \\ m_{21} & m_{22} & m_{23} & 0 & 0 & 0 & 0 \\ m_{31} & m_{32} & m_{33} & 0 & 0 & 0 & 0 \\ 0 & 0 & 0 & m_{44} & 0 & 0 & 0 \\ 0 & 0 & 0 & 0 & m_{55} & 0 & 0 \\ 0 & 0 & 0 & 0 & 0 & m_{66} & 0 \\ 0 & 0 & 0 & 0 & 0 & 0 & m_{77} \end{pmatrix}, \tag{16}$$

with

$$m_{11} = m + \frac{I_{G\beta}}{{l_t}^2} \qquad m_{12} = -\frac{I_{G\beta}\, w_d}{W\, {l_t}^2} \tag{17}$$

$$m_{13} = -\frac{I_{G\beta}\, w_i}{W\, {l_t}^2} \qquad m_{22} = \frac{I_{G\alpha}\, {l_t}^2 + I_{G\beta}\, {w_d}^2}{W^2\, {l_t}^2} \tag{18}$$

$$m_{23} = -\frac{I_{G\alpha}\, {l_t}^2 - I_{G\beta}\, w_d\, w_i}{W^2\, {l_t}^2} \qquad m_{33} = \frac{I_{G\alpha}\, {l_t}^2 + I_{G\beta}\, {w_i}^2}{W^2\, {l_t}^2} \tag{19}$$

$$m_{44} = m_{ssdi} \qquad m_{55} = m_{ssdd} \tag{20}$$

$$m_{66} = m_{ssti} \qquad m_{77} = m_{sstd} \tag{21}$$

where m is the mass of the main frame, $I_{G\alpha}$ and $I_{G\beta}$ are the roll and pitch moments of inertia of the main frame, $L = l_t + l_d$ is the wheelbase, W is the track width, l_d and l_t are the distances from the centre of mass to the front and rear axles, respectively, and w_i and w_d are the left and right half track width.

The symmetric damping matrix is obtained as follows:

$$\boldsymbol{D} = \begin{pmatrix} d_{11} & d_{12} & d_{13} & d_{14} & d_{15} & 0 & 0 \\ d_{21} & d_{22} & d_{23} & d_{24} & d_{25} & d_{26} & 0 \\ d_{31} & d_{32} & d_{33} & d_{34} & d_{35} & 0 & d_{37} \\ d_{41} & d_{42} & d_{43} & d_{44} & 0 & 0 & 0 \\ d_{51} & d_{52} & d_{53} & 0 & d_{55} & 0 & 0 \\ 0 & d_{62} & 0 & 0 & 0 & d_{66} & d_{67} \\ 0 & 0 & d_{73} & 0 & 0 & d_{76} & d_{77} \end{pmatrix}, \tag{22}$$

with

$$d_{11} = \frac{L^2\, d_{sdd}}{{l_t}^2} + \frac{L^2\, d_{sdi}}{{l_t}^2} \tag{23}$$

$$d_{12} = \frac{L\, d_{sdi}\, w_i}{W\, l_t} - \frac{L\, d_{sdd}\, w_d}{W\, l_t} - \frac{L\, d_{sdd}\, l_d\, w_d}{W\, {l_t}^2} - \frac{L\, d_{sdi}\, l_d\, w_d}{W\, {l_t}^2} \tag{24}$$

$$d_{13} = \frac{L\, d_{sdd}\, w_d}{W\, l_t} - \frac{L\, d_{sdi}\, w_i}{W\, l_t} - \frac{L\, d_{sdd}\, l_d\, w_i}{W\, {l_t}^2} - \frac{L\, d_{sdi}\, l_d\, w_i}{W\, {l_t}^2} \tag{25}$$

$$d_{14} = -\frac{L\, d_{sdi}}{l_t} \tag{26}$$

$$d_{15} = -\frac{L\, d_{sdd}}{l_t} \tag{27}$$

$$d_{22} = d_{sti} + \frac{d_{sdi}\, {w_i}^2}{W^2} + \frac{L^2\, d_{sdd}\, {w_d}^2}{W^2\, {l_t}^2} + \frac{d_{sdi}\, {l_d}^2\, {w_d}^2}{W^2\, {l_t}^2} - \frac{2\, d_{sdi}\, l_d\, w_d\, w_i}{W^2\, l_t} \tag{28}$$

$$d_{23} = \frac{L\, d_{sdd}\, l_d\, w_d\, w_i}{W^2\, {l_t}^2} - \frac{L\, d_{sdi}\, {w_i}^2}{W^2\, l_t} - \frac{L\, d_{sdd}\, {w_d}^2}{W^2\, l_t} + \frac{L\, d_{sdi}\, l_d\, w_d\, w_i}{W^2\, {l_t}^2} \tag{29}$$

$$d_{24} = \frac{d_{sdi}\, l_d\, w_d}{W\, l_t} - \frac{d_{sdi}\, w_i}{W} \tag{30}$$

$$d_{25} = \frac{L\, d_{sdd}\, w_d}{W\, l_t} \tag{31}$$

$$d_{26} = -d_{sti} \tag{32}$$

$$d_{33} = d_{std} + \frac{d_{sdd}\, {w_d}^2}{W^2} + \frac{L^2\, d_{sdi}\, {w_i}^2}{W^2\, {l_t}^2} + \frac{d_{sdd}\, {l_d}^2\, {w_i}^2}{W^2\, {l_t}^2} - \frac{2\, d_{sdd}\, l_d\, w_d\, w_i}{W^2\, l_t} \tag{33}$$

$$d_{34} = \frac{L\, d_{sdi}\, w_i}{W\, l_t} \tag{34}$$

$$d_{35} = \frac{d_{sdd}\, l_d\, w_i}{W\, l_t} - \frac{d_{sdd}\, w_d}{W} \tag{35}$$

$$d_{37} = -d_{std} \tag{36}$$

$$d_{44} = d_{rdi} + d_{sdi} \tag{37}$$

$$d_{55} = d_{rdd} + d_{sdd} \tag{38}$$

$$d_{66} = d_{rti} + d_{sti} + d_{tb} \tag{39}$$

$$d_{67} = -d_{tb} \tag{40}$$

$$d_{77} = d_{rtd} + d_{std} + d_{tb} \tag{41}$$

In the previous matrix, d_{sdi}, d_{sdd}, d_{sti} and d_{std} are the damping constants of the left front, right front, left rear and right rear suspension dampers, respectively, d_{rdi}, d_{rdd}, d_{rti} and d_{rtd} are the damping constants of the left front, right front, left rear and right rear wheel dampers, respectively, and d_{tb} is the damping constant of the torsion bar.

The stiffness matrix is also symmetric and can be expressed as follows

$$\boldsymbol{K} = \begin{pmatrix} k_{11} & k_{12} & k_{13} & k_{14} & k_{15} & 0 & 0 \\ k_{21} & k_{22} & k_{23} & k_{24} & k_{25} & k_{26} & 0 \\ k_{31} & k_{32} & k_{33} & k_{34} & k_{35} & 0 & k_{37} \\ k_{41} & k_{42} & k_{43} & k_{44} & 0 & 0 & 0 \\ k_{51} & k_{52} & k_{53} & 0 & k_{55} & 0 & 0 \\ 0 & k_{62} & 0 & 0 & 0 & k_{66} & k_{67} \\ 0 & 0 & k_{73} & 0 & 0 & k_{76} & k_{77} \end{pmatrix}, \tag{42}$$

where the elements of the matrix can be obtained by replacing in Eqs. (23)–(41) each damping coefficient by its parallel spring stiffness coefficient according to Fig. 5. In the resulting expressions, the model parameters k_{sdi}, k_{sdd}, k_{sti} and k_{std} are the stiffness

constants of the left front, right front, left rear and right rear suspension springs, respectively, k_{rdi}, k_{rdd}, k_{rti} and k_{rtd} are the stiffness constants of the left front, right front, left rear and right rear wheel spring, respectively, and k_{tb} is the stiffness constant of the torsion bar.

Finally, the vector of gravitational forces reads as

$$\boldsymbol{f}_g = \begin{pmatrix} -g\,m \\ 0 \\ 0 \\ -g\,m_{ssdi} \\ -g\,m_{ssdd} \\ -g\,m_{ssti} \\ -g\,m_{sstd} \end{pmatrix}. \tag{43}$$

while the vector of forces induced by the ground unevenness reads as

$$\boldsymbol{f}_y = \begin{pmatrix} 0 \\ 0 \\ 0 \\ d_{rdi}\,\dot{y}_{di} + k_{rdi}\,y_{di} \\ d_{rdd}\,\dot{y}_{dd} + k_{rdd}\,y_{dd} \\ d_{rti}\,\dot{y}_{ti} + k_{rti}\,y_{ti} \\ d_{rtd}\,\dot{y}_{td} + k_{rtd}\,y_{td} \end{pmatrix}. \tag{44}$$

It shall be noted that the mass, damping and stiffness matrices resulting from the selection of displacement coordinates shown in Eq. (14) are all non-diagonal, showing inertial, damping and elastic coupling.

3.1.2. Using translational and rotational coordinates

In a second approach, as stated above, it is common in vertical dynamic analysis of vehicles to use a set of mixed translational and angular coordinates. Following this approach, the new vector of generalized coordinates is

$$\boldsymbol{x} = \begin{pmatrix} x & \alpha & \beta & x_{di} & x_{dd} & x_{ti} & x_{td} \end{pmatrix}^T \tag{45}$$

Now, as explained in Section 2.2.2, two fictitious displacement coordinates are introduced,

$$x_\alpha = W\alpha, \quad x_\beta = L\beta. \tag{46}$$

where L is the wheelbase and W is the track width (see Fig. 5). Then, repeating the previous process, the equation of motion can be obtained for the following set of generalized coordinates:

$$\boldsymbol{x} = \begin{pmatrix} x & x_\alpha & x_\beta & x_{di} & x_{dd} & x_{ti} & x_{td} \end{pmatrix}^T \tag{47}$$

This set of generalized coordinates leads to new matrices with different structures than those obtained using only translational coordinates:

$$\boldsymbol{M} = \begin{pmatrix} m_{11} & 0 & 0 & 0 & 0 & 0 & 0 \\ 0 & m_{22} & 0 & 0 & 0 & 0 & 0 \\ 0 & 0 & m_{33} & 0 & 0 & 0 & 0 \\ 0 & 0 & 0 & m_{44} & 0 & 0 & 0 \\ 0 & 0 & 0 & 0 & m_{55} & 0 & 0 \\ 0 & 0 & 0 & 0 & 0 & m_{66} & 0 \\ 0 & 0 & 0 & 0 & 0 & 0 & m_{77} \end{pmatrix}, \tag{48}$$

$$\boldsymbol{D} = \begin{pmatrix} d_{11} & d_{12} & d_{13} & d_{14} & d_{15} & d_{16} & d_{17} \\ d_{21} & d_{22} & d_{23} & d_{24} & d_{25} & d_{26} & d_{27} \\ d_{31} & d_{32} & d_{33} & d_{34} & d_{35} & d_{36} & d_{37} \\ d_{41} & d_{42} & d_{43} & d_{44} & 0 & 0 & 0 \\ d_{51} & d_{52} & d_{53} & 0 & d_{55} & 0 & 0 \\ d_{61} & d_{62} & d_{63} & 0 & 0 & d_{66} & d_{67} \\ d_{71} & d_{72} & d_{73} & 0 & 0 & d_{76} & d_{77} \end{pmatrix}, \tag{49}$$

$$\boldsymbol{K} = \begin{pmatrix} k_{11} & k_{12} & k_{13} & k_{14} & k_{15} & k_{16} & k_{17} \\ k_{21} & k_{22} & k_{23} & k_{24} & k_{25} & k_{26} & k_{27} \\ k_{31} & k_{32} & k_{33} & k_{34} & k_{35} & k_{36} & k_{37} \\ k_{41} & k_{42} & k_{43} & k_{44} & 0 & 0 & 0 \\ k_{51} & k_{52} & k_{53} & 0 & k_{55} & 0 & 0 \\ k_{61} & k_{62} & k_{63} & 0 & 0 & k_{66} & k_{67} \\ k_{71} & k_{72} & k_{73} & 0 & 0 & k_{76} & k_{77} \end{pmatrix}, \tag{50}$$

It is interesting to note that the mass matrix is now diagonal, therefore removing the inertial coupling. The value of the elements of these mass, damping and stiffness matrices obtained for the set of mixed coordinates are detailed in Appendix A.

Using this set of coordinates, vectors $\boldsymbol{f}_g$ and $\boldsymbol{f}_y$ are identical to those of Eqs. (43) and (44), respectively.

3.2. Electrical analogue of the full car

Once the differential equations that model the vertical dynamics of the car are derived, the second step of the procedure to obtain the electrical analogue is applied. As stated previously, unlike traditional approaches in which an attempt is made to establish the structure of the electrical circuit by analogy with the mechanical one, the method proposed in this paper first establishes the equations in both domains and then finds the appropriate structure of the electrical circuit.

3.2.1. Model based on translational coordinates only

Applying the force–current analogy according to Table 2, matrices $\boldsymbol{C}$, $\boldsymbol{G}$ and $\boldsymbol{B}$ are identical to matrices $\boldsymbol{M}$, $\boldsymbol{D}$ and $\boldsymbol{K}$ defined in Section 3.1.1 for the set of translational coordinates. Thus, the components of matrices $\boldsymbol{C}$, $\boldsymbol{G}$ and $\boldsymbol{B}$ are obtained using the following relationships: $c_{jk} = m_{jk}$, $g_{jk} = d_{jk}$ and $b_{jk} = k_{jk}$.

The values for the elements of each of these matrices are also defined in Section 3.1.1. Based on this matrix structure, following the node-voltage method, an electric circuit can be synthesized as shown in Fig. 6, where, the values of the electrical elements connected between non-ground nodes are

$$C_{jk} = -c_{jk}, \qquad G_{jk} = -g_{jk}, \qquad B_{jk} = -b_{jk} \tag{51}$$

The electrical elements connected to the ground are obtained as

$$C_j = \sum_{k=1}^{7} c_{jk}, \qquad G_j = \sum_{k=1}^{7} g_{jk}, \qquad B_j = \sum_{k=1}^{7} c_{jk} \tag{52}$$

resulting in the following values expressed in terms of mechanical coefficients:

$$\begin{aligned}
&C_1 = m && G_4 = d_{rdi} && B_4 = k_{rdi}\\
&C_4 = m_{ssdi} && G_5 = d_{rdd} && B_5 = k_{rdd}\\
&C_5 = m_{ssdd} && G_6 = d_{rti} && B_6 = k_{rti}\\
&C_6 = m_{ssti} && G_7 = d_{rtd} && B_7 = k_{rtd}\\
&C_7 = m_{sstd}
\end{aligned}$$

It must be noted that some of the possible electrical elements connected to the ground result in a zero value after adding up all elements in the corresponding row of the matrix, and have not been included in the above list nor drawn in Fig. 6.

Finally, the current source vector $\boldsymbol{i}$ takes the value of the force vector $\boldsymbol{f}_g + \boldsymbol{f}_y$ (see Eqs. (43) and (44)).

3.2.2. Model based on translational and rotational coordinates

In the following, the electrical analogue of the car is considered for the set of mixed translational and rotational coordinates. According to the force–current analogy, matrices $\boldsymbol{C}$, $\boldsymbol{G}$ and $\boldsymbol{B}$ are identical to matrices $\boldsymbol{M}$, $\boldsymbol{D}$ and $\boldsymbol{K}$ defined in Section 3.1.2. Therefore, the following identities hold among the elements of the matrices: $c_{jk} = m_{jk}$, $g_{jk} = d_{jk}$ and $b_{jk} = k_{jk}$. See Appendix A for the value of the mechanical coefficients.

Applying the node-voltage method, the values of the electrical elements connected between non-ground nodes are obtained from Eq. (51). Similarly, the electrical elements connected to the ground are obtained from Eq. (52). The resulting values expressed in terms of mechanical coefficients are detailed in Appendix B. In contrast to the matrices obtained using only translation coordinates, mixed coordinates lead to a larger number of electrical elements and connections between nodes (6 more branches), resulting in a more complicated electrical circuit than the previous one shown in Fig. 6. This electrical circuit has not been drawn here, but it can be easily built following the node-voltage method.

3.3. Harmonic analysis in the frequency domain

Once the dynamics have been defined through the system of equations in the electrical domain, the harmonic analysis in the frequency domain can be carried out using phasors as detailed in [13]. The mapping of variables from the time domain to the complex domain is specified in Table 3. This results in a system of linear equations in complex variable

$$[\vec{Y}][\vec{U}] = [\vec{I}] \qquad \rightarrow \qquad [\vec{U}] = [\vec{Y}]^{-1}[\vec{I}] \tag{53}$$

where the matrix $[\vec{Y}]$ includes the complex admittances of the circuit, while $[\vec{U}]$ and $[\vec{I}]$ are the voltage and current phasor vectors, respectively. To solve the problem, the admittance matrix is inverted, thus providing the voltage values at every node of the electrical circuit. Once the voltages have been determined, the remaining currents can be found. In this way, the analogy can be undone and the velocities and forces in the mechanical system can be obtained.

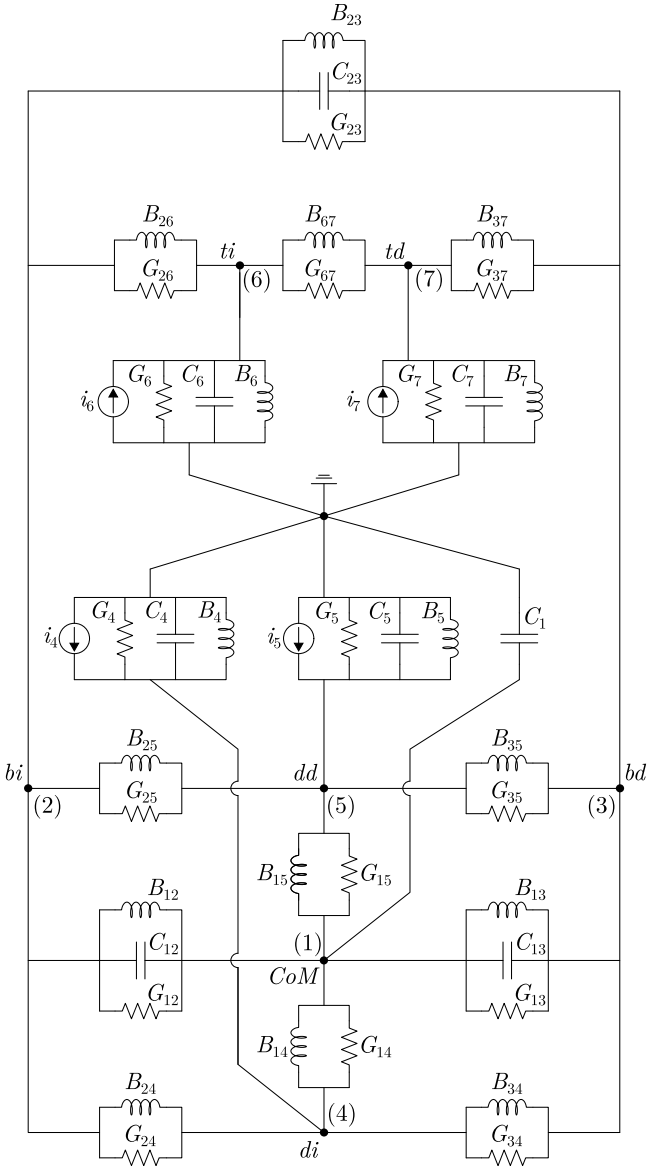

Fig. 6. 7-DOF electric circuit for the full car model.

Table 3
Complex-valued equivalents of passive electrical linear elements.

Time domain		Phasor Domain	
Element	Symbol	Admittance	Impedance
Capacitor	C	$\vec{B}_C = C\omega j$	$\vec{X}_C = \frac{1}{\vec{B}_C}$
Inductor	L	$\vec{B}_L = \frac{1}{\vec{X}_L}$	$\vec{X}_L = L\omega j$
Resistor	R	G	$R = \frac{1}{G}$
Series	$R + L + C$	$\vec{Y} = \frac{1}{\vec{Z}}$	$\vec{Z} = R + Xj$
Parallel	$R /\!/ L /\!/ C$	$\vec{Y} = G + Bj$	$\vec{Z} = \frac{1}{\vec{Y}}$

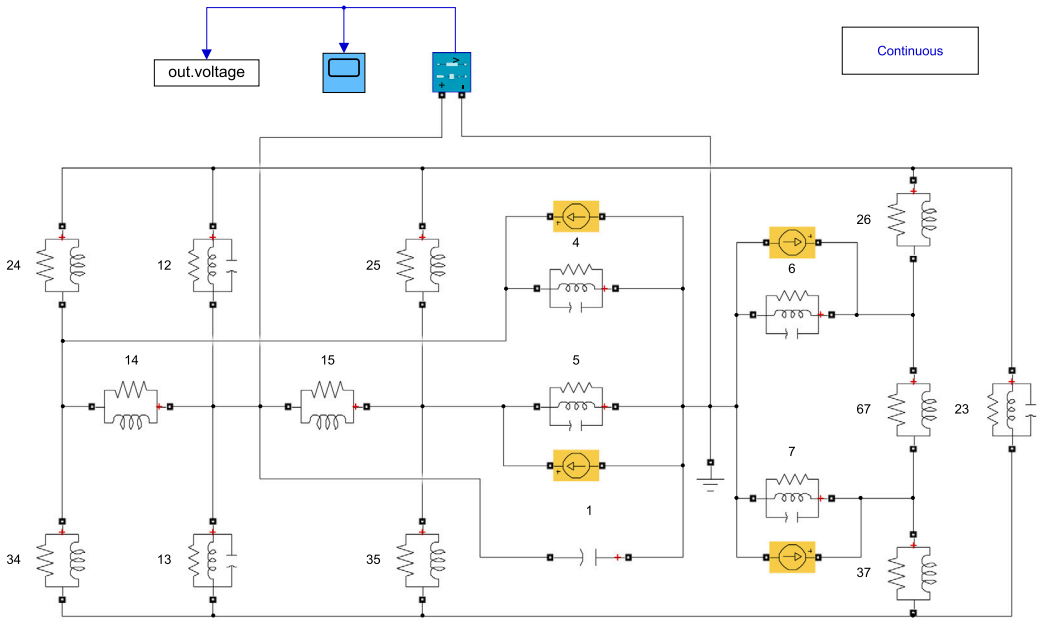

Fig. 7. Simulink model of the electric circuit analogue presented in Fig. 6.

4. Numerical results and validation

This section presents a validation of the electrical analogue of the linear 7-DOF full car model. The validation is done in such a way that the results of the mechanical model, obtained using regular linear mechanical system techniques, are compared to those of the electrical circuit drawn in Fig. 6, which are obtained using the well-known software Simulink by Matlab′. The mechanical properties of the three-dimensional full car model are collected in Table 4, which are mainly taken from Ref. [65].

The type of analysis carried out is a harmonic steady-state vibration analysis in which the car model is assumed to travel with a forward speed $v = 100$ km/h on an uneven road having a harmonic profile characterized by a wavelength $\lambda = 2$ m and amplitude $Y = 5$ cm. In addition, the right wheels are assumed to experience harmonic unevenness with a phase shift, $t_\phi = 0.0540$ s with respect to the left wheels. Thus, the time-dependent functions $y_{di}(t)$, $y_{dd}(t)$, $y_{ti}(t)$ and $y_{td}(t)$ read as follows:

$$y_{di}(t) = Y \sin(\omega t) \tag{54}$$

$$y_{dd}(t) = Y \sin\left(\omega\left(t - t_\phi\right)\right) \tag{55}$$

$$y_{ti}(t) = Y \sin\left(\omega t - \phi_L\right) \tag{56}$$

$$y_{td}(t) = Y \sin\left(\omega\left(t - t_\phi\right) - \phi_L\right) \tag{57}$$

where $\omega = \dfrac{2\pi v}{\lambda}$ and $\phi_L = \dfrac{2\pi L}{\lambda}$.

The reason for using a harmonic excitation for validation purposes in this work is twofold. On the one hand, the harmonic excitation can be seen as an elementary excitation that is used to construct more complex excitations by using the discrete Fourier transform in linear systems, since the superposition principle is applicable. Therefore, the electrical analogue can also be used with more complex excitations, i.e. with random excitations. On the other hand, the harmonic excitation is sufficient to obtain results that allow the conclusion that the electrical circuit and the mechanical system are, in fact, analogous to each other.

Eq. (15) can be rewritten without the constant gravitational force term, $\boldsymbol{f}_g$, by defining a coordinate transformation, $\boldsymbol{x} = \boldsymbol{x}_1 + \boldsymbol{k}^{-1}\boldsymbol{f}_g$, that translate the origin of the coordinate system to a vertical equilibrium position. This way, the equations of motion can be written more simply as

$$\boldsymbol{M}\ddot{\boldsymbol{x}}_1 + \boldsymbol{D}\dot{\boldsymbol{x}}_1 + \boldsymbol{K}\boldsymbol{x}_1 = \boldsymbol{f}_y(t) \tag{58}$$

where

$$\boldsymbol{x}_1 = \begin{pmatrix} x_1 & x_{bi1} & x_{bd1} & x_{di1} & x_{dd1} & x_{ti1} & x_{td1} \end{pmatrix}^T \tag{59}$$

As is usual in harmonic analysis of linear systems, the sinusoidal functions in Eqs. (54)–(57) can be substituted by complex exponentials with frequency ω. This way, the term $\boldsymbol{f}_y(t)$ can be written as

$$\boldsymbol{f}_y(t) = \boldsymbol{f}_0 e^{i\omega t}, \quad \boldsymbol{f}_0 \in \mathbb{C}^n \tag{60}$$

Table 4
Mechanical properties of the car model.

Parameter	Symbol	Value	Units
mass of the main frame	m	1500	kg
pitch moment of inertia	$I_{G\beta}$	2160	kgm^2
roll moment of inertia	$I_{G\alpha}$	1500	kgm^2
unsprung mass of the left front wheel	m_{ssdi}	70	kg
unsprung mass of the right front wheel	m_{ssdd}	70	kg
unsprung mass of the left rear wheel	m_{ssti}	60	kg
unsprung mass of the right rear wheel	m_{sstd}	60	kg
stiffness of the left front suspension	k_{sdi}	35000	N/m
stiffness of the right front suspension	k_{sdd}	35000	N/m
stiffness of the left rear suspension	k_{sti}	38000	N/m
stiffness of the right rear suspension	k_{std}	38000	N/m
stiffness of the torsion bar	k_{tb}	20000	N/m
damping of the left front suspension	d_{sdi}	1000	Ns/m
damping of the right front suspension	d_{sdd}	1000	Ns/m
damping of the left rear suspension	d_{sti}	1100	Ns/m
damping of the right rear suspension	d_{std}	1100	Ns/m
damping of the torsion bar	d_{tb}	100	Ns/m
stiffness of the left front wheel	k_{rdi}	190000	N/m
stiffness of the right front wheel	k_{rdd}	190000	N/m
stiffness of the left rear wheel	k_{rti}	190000	N/m
stiffness of the right rear wheel	k_{rtd}	190000	N/m
damping of the left front wheel	d_{rdi}	50	Ns/m
damping of the right front wheel	d_{rdd}	50	Ns/m
damping of the left rear wheel	d_{rti}	50	Ns/m
damping of the right rear wheel	d_{rtd}	50	Ns/m
centre of mass to front axle distance	l_d	1.2	m
centre of mass to rear axle distance	l_t	1.59	m
left half track width	w_i	0.78	m
right half track width	w_d	0.78	m
track width	$W = w_i + w_d$	1.56	m
wheelbase	$L = l_d + l_t$	2.79	m

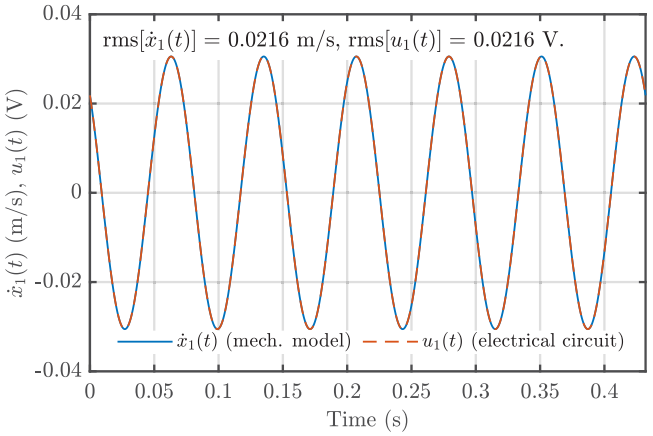

Fig. 8. Vertical velocity of the vehicle's centre of mass, $\dot{x}_1(t)$, calculated by solving the mechanical model as per Eq. (61) and by measuring the voltage of node 1 of the electric analogue, $u_1(t)$, shown in Fig. 6.

Then, the steady-state response can be obtained as the imaginary part of the following complex vector

$$\boldsymbol{x}_1(t) = \boldsymbol{H}(\omega)\, \boldsymbol{f}_0 \mathrm{e}^{\mathrm{i}\omega t}, \tag{61}$$

where $\boldsymbol{H}(\omega) = \left(-\omega^2 \boldsymbol{M} + \mathrm{i}\omega \boldsymbol{C} + \boldsymbol{K}\right)^{-1}$.

The result for the vertical velocity of the vehicle's centre of mass (CoM) $\dot{x}_1(t)$ is shown in Fig. 8. It has been computed by solving the mechanical model as per Eq. (61). This figure also plots the same velocity computed by measuring the voltage of node 1 $u_1(t)$ in the electric analogue shown in Fig. 6. The Simulink model is shown in Fig. 7. The RMS values of velocity $\dot{x}_1(t)$ and voltage $u_1(t)$ are also shown in Fig. 8. It can be seen that both, velocity profiles and RMS values, match perfectly.

5. Discussion

The methodology described makes use of well-known methods from both the mechanical and electrical engineering fields, making the application of the proposed method more simple than the existing rules for obtaining electrical analogues of linear mechanical systems on an element-by-element basis. In essence, the method consists of obtaining the dynamic equations of the mechanical system in matrix form, translating these equations to the electrical domain, and finally getting the electrical circuit by direct inspection of the matrices. To the author's knowledge, this procedure has not been previously found in the literature. In addition, the method is equally applicable to both force–current and force–voltage analogies. The selection of one method or the other will result in two different but dual circuits. The proposed methodology has the advantage of being applicable to complex mechanical systems, with inertial, elastic, and damping coupling. It can also deal with translational, rotational, or a combination of translational and rotational coordinates.

To prove the feasibility of the methodology, an electrical analogue of a 3D 7-DOF linear full car model is obtained and validated through numerical results. Since in the existing literature only electrical analogues of quarter car and half car models have been reported, the electrical analogue of a full car is a main contribution of this work, which is expected to be useful in future studies related to active suspension and energy harvesters. From the complexity of the resulting analog electric circuit of the full car model and, especially, from the values of the electrical elements reported in the appendices of this paper, it is easy to understand the great difficulty of arriving at this solution by applying the traditional rules.

The methodology proposed in this paper is different to that of Bond Graph method since it aims at finding an electrical analogue of a mechanical system rather than combining the dynamic equations of the mechanical and the electrical components. This may be useful for researchers working with electrical analogues of mechanical systems in the electrical domain. The proposed methodology does not grow in complexity when the topology of the mechanical system becomes more involved as it works directly on the system matrices, which can be large or small but will always be two-dimensional array data structures. The use of electrical analogues leads to a direct and straightforward solution for the dynamics of the whole electromechanical problem in the electrical domain, where it is sufficient to apply the well-known techniques of circuit analysis without the need for additional new knowledge. Furthermore, there is no need to deal neither with causalities issues nor exponential growth in the complexity of the system topology while keeping simplicity at a minimum.

In addition to the described benefits of the proposed methodology, another advantage is its feasibility to be implemented in specific software for the construction of electromechanical analogues, which would enhance the use of analogues in the different fields.

6. Summary and conclusions

This work has presented a general and systematic methodology to obtain electrical analogues of any linear model of a mechanical system. The method can be described in a few simple steps.

The model's equations of motion are first determined and written in matrix form in the mechanical domain. This stage can be carried out using any of the Classical Mechanics methods already available. The coordinates of the model must be homogeneous, which means that they can only be of one type – translational or rotational – but not both. This also implies homogeneity of the differential equations, which can be either force or moment equations. If the original set of coordinates chosen when modelling the system includes translational or rotational coordinates, they can easily be homogenized using length scale factors. The mechanical matrices of the dynamic model are used to identify the electrical matrices in the second stage, exploiting the analogy between the mechanical and electrical domains. Finally, in the third phase, the analogue circuit is developed in the electrical domain using well-known methods in network analysis like node-voltage or mesh-current, depending on the analogy used. Once the method has been described, a simple 2-DOF mechanical model is used to illustrate the application of the proposed methodology in detail.

To demonstrate the general applicability of the method, the electric analogue of a linear 7-DOF full car model is obtained, which to the best of the authors' knowledge was never published before. The electric analogue has been validated through a comparison of the results from simulations of both the mechanical and the electrical models.

The main conclusions of this work are as follows:

(i) A complete and systematic methodology has been presented to obtain the electrical analogue of linear mechanical systems of any level of complexity modelled by rigid bodies, springs and dampers.
(ii) The proposed methodology is straightforward and simple, and can be used in mechanical models that include a combination of translational and rotational coordinates.
(iii) The electrical analogue of a 3D 7-DOF linear model of a complete car has been developed. This model is one of the main contributions of this work and has exemplified the potential of the method in its application to complex mechanical systems.

The framework presented here is expected to help mechatronic engineers to analyse and design newly optimized and improved electromechanical components for vehicles and other mechatronic systems.

As a future research direction, the automatic generation of the electrical analogue of any arbitrary mechanical system from its inertia, damping and stiffness matrices based on the presented methodology is envisaged.

Declaration of competing interest

The authors declare that they have no known competing financial interests or personal relationships that could have appeared to influence the work reported in this paper.

Acknowledgements

This work was partially supported by the Ministry of Science and Innovation, Spain under Grant PGC2018-098813-B-C33.

Appendix A. Mechanical matrices of the full car for the set of translational and rotational coordinates

This appendix details the values of the mass, damping and stiffness matrices of the full car obtained for the set of generalized coordinates (see Section 3.1.2):

$$\boldsymbol{x} = \begin{pmatrix} x & x_\alpha & x_\beta & x_{di} & x_{dd} & x_{ti} & x_{td} \end{pmatrix}^T \tag{A.1}$$

The mass matrix results in a diagonal matrix:

$$\boldsymbol{M} = \begin{pmatrix} m_{11} & 0 & 0 & 0 & 0 & 0 & 0 \\ 0 & m_{22} & 0 & 0 & 0 & 0 & 0 \\ 0 & 0 & m_{33} & 0 & 0 & 0 & 0 \\ 0 & 0 & 0 & m_{44} & 0 & 0 & 0 \\ 0 & 0 & 0 & 0 & m_{55} & 0 & 0 \\ 0 & 0 & 0 & 0 & 0 & m_{66} & 0 \\ 0 & 0 & 0 & 0 & 0 & 0 & m_{77} \end{pmatrix}, \tag{A.2}$$

with

$$m_{11} = m \tag{A.3}$$
$$m_{22} = \frac{I_{G\alpha}}{W^2} \tag{A.4}$$
$$m_{33} = \frac{I_{G\beta}}{L^2} \tag{A.5}$$
$$m_{44} = m_{ssdi} \tag{A.6}$$
$$m_{55} = m_{ssdd} \tag{A.7}$$
$$m_{66} = m_{ssti} \tag{A.8}$$
$$m_{77} = m_{sstd} \tag{A.9}$$

The symmetric damping matrix is as follows:

$$\boldsymbol{D} = \begin{pmatrix} d_{11} & d_{12} & d_{13} & d_{14} & d_{15} & d_{16} & d_{17} \\ d_{21} & d_{22} & d_{23} & d_{24} & d_{25} & d_{26} & d_{27} \\ d_{31} & d_{32} & d_{33} & d_{34} & d_{35} & d_{36} & d_{37} \\ d_{41} & d_{42} & d_{43} & d_{44} & 0 & 0 & 0 \\ d_{51} & d_{52} & d_{53} & 0 & d_{55} & 0 & 0 \\ d_{61} & d_{62} & d_{63} & 0 & 0 & d_{66} & d_{67} \\ d_{71} & d_{72} & d_{73} & 0 & 0 & d_{76} & d_{77} \end{pmatrix}, \tag{A.10}$$

with

$$d_{11} = d_{sdd} + d_{sdi} + d_{std} + d_{sti} \tag{A.11}$$
$$d_{12} = \frac{d_{sdi}\, w_i}{W} - \frac{d_{std}\, w_d}{W} - \frac{d_{sdd}\, w_d}{W} + \frac{d_{sti}\, w_i}{W} \tag{A.12}$$
$$d_{13} = \frac{d_{std}\, l_t}{L} - \frac{d_{sdi}\, l_d}{L} - \frac{d_{sdd}\, l_d}{L} + \frac{d_{sti}\, l_t}{L} \tag{A.13}$$
$$d_{14} = -d_{sdi} \tag{A.14}$$
$$d_{15} = -d_{sdd} \tag{A.15}$$
$$d_{16} = -d_{sti} \tag{A.16}$$
$$d_{17} = -d_{std} \tag{A.17}$$
$$d_{22} = \frac{d_{sdd}\, {w_d}^2}{W^2} + \frac{d_{std}\, {w_d}^2}{W^2} + \frac{d_{sdi}\, {w_i}^2}{W^2} + \frac{d_{sti}\, {w_i}^2}{W^2} \tag{A.18}$$

$$d_{23} = \frac{d_{sdd}\, l_d\, w_d}{L\, W} - \frac{d_{sdi}\, l_d\, w_i}{L\, W} - \frac{d_{std}\, l_t\, w_d}{L\, W} + \frac{d_{sti}\, l_t\, w_i}{L\, W} \tag{A.19}$$

$$d_{24} = -\frac{d_{sdi}\, w_i}{W} \tag{A.20}$$

$$d_{25} = \frac{d_{sdd}\, w_d}{W} \tag{A.21}$$

$$d_{26} = -\frac{d_{sti}\, w_i}{W} \tag{A.22}$$

$$d_{27} = \frac{d_{std}\, w_d}{W} \tag{A.23}$$

$$d_{33} = \frac{d_{sdd}\, {l_d}^2}{L^2} + \frac{d_{sdi}\, {l_d}^2}{L^2} + \frac{d_{std}\, {l_t}^2}{L^2} + \frac{d_{sti}\, {l_t}^2}{L^2} \tag{A.24}$$

$$d_{34} = \frac{d_{sdi}\, l_d}{L} \tag{A.25}$$

$$d_{35} = \frac{d_{sdd}\, l_d}{L} \tag{A.26}$$

$$d_{36} = -\frac{d_{sti}\, l_t}{L} \tag{A.27}$$

$$d_{37} = -\frac{d_{std}\, l_t}{L} \tag{A.28}$$

$$d_{44} = d_{rdi} + d_{sdi} \tag{A.29}$$

$$d_{55} = d_{rdd} + d_{sdd} \tag{A.30}$$

$$d_{66} = d_{rti} + d_{sti} + d_{tb} \tag{A.31}$$

$$d_{67} = -d_{tb} \tag{A.32}$$

$$d_{77} = d_{rtd} + d_{std} + d_{tb} \tag{A.33}$$

Finally, the stiffness matrix is as follows:

$$\boldsymbol{K} = \begin{pmatrix} k_{11} & k_{12} & k_{13} & k_{14} & k_{15} & k_{16} & k_{17} \\ k_{21} & k_{22} & k_{23} & k_{24} & k_{25} & k_{26} & k_{27} \\ k_{31} & k_{32} & k_{33} & k_{34} & k_{35} & k_{36} & k_{37} \\ k_{41} & k_{42} & k_{43} & k_{44} & 0 & 0 & 0 \\ k_{51} & k_{52} & k_{53} & 0 & k_{55} & 0 & 0 \\ k_{61} & k_{62} & k_{63} & 0 & 0 & k_{66} & k_{67} \\ k_{71} & k_{72} & k_{73} & 0 & 0 & k_{76} & k_{77} \end{pmatrix}, \tag{A.34}$$

with

$$k_{11} = k_{sdd} + k_{sdi} + k_{std} + k_{sti} \tag{A.35}$$

$$k_{12} = \frac{k_{sdi}\, w_i}{W} - \frac{k_{std}\, w_d}{W} - \frac{k_{sdd}\, w_d}{W} + \frac{k_{sti}\, w_i}{W} \tag{A.36}$$

$$k_{13} = \frac{k_{std}\, l_t}{L} - \frac{k_{sdi}\, l_d}{L} - \frac{k_{sdd}\, l_d}{L} + \frac{k_{sti}\, l_t}{L} \tag{A.37}$$

$$k_{14} = -k_{sdi} \tag{A.38}$$

$$k_{15} = -k_{sdd} \tag{A.39}$$

$$k_{16} = -k_{sti} \tag{A.40}$$

$$k_{17} = -k_{std} \tag{A.41}$$

$$k_{22} = \frac{k_{sdd}\, {w_d}^2}{W^2} + \frac{k_{std}\, {w_d}^2}{W^2} + \frac{k_{sdi}\, {w_i}^2}{W^2} + \frac{k_{sti}\, {w_i}^2}{W^2} \tag{A.42}$$

$$k_{23} = \frac{k_{sdd}\, l_d\, w_d}{L\, W} - \frac{k_{sdi}\, l_d\, w_i}{L\, W} - \frac{k_{std}\, l_t\, w_d}{L\, W} + \frac{k_{sti}\, l_t\, w_i}{L\, W} \tag{A.43}$$

$$k_{24} = -\frac{k_{sdi}\, w_i}{W} \tag{A.44}$$

$$k_{25} = \frac{k_{sdd}\, w_d}{W} \tag{A.45}$$

$$k_{26} = -\frac{k_{sti}\, w_i}{W} \tag{A.46}$$

$$k_{27} = \frac{k_{std}\, w_d}{W} \tag{A.47}$$

$$k_{33} = \frac{k_{sdd}\, {l_d}^2}{L^2} + \frac{k_{sdi}\, {l_d}^2}{L^2} + \frac{k_{std}\, {l_t}^2}{L^2} + \frac{k_{sti}\, {l_t}^2}{L^2} \tag{A.48}$$

$$k_{34} = \frac{k_{sdi}\, l_d}{L} \tag{A.49}$$

$$k_{35} = \frac{k_{sdd}\, l_d}{L} \tag{A.50}$$

$$k_{36} = -\frac{k_{sti}\, l_t}{L} \tag{A.51}$$

$$k_{37} = -\frac{k_{std}\, l_t}{L} \tag{A.52}$$

$$k_{44} = k_{rdi} + k_{sdi} \tag{A.53}$$

$$k_{55} = k_{rdd} + k_{sdd} \tag{A.54}$$

$$k_{66} = k_{rti} + k_{sti} + k_{tb} \tag{A.55}$$

$$k_{67} = -k_{tb} \tag{A.56}$$

$$k_{77} = k_{rtd} + k_{std} + k_{tb} \tag{A.57}$$

Appendix B. Electrical elements obtained from the node-voltage method for the full car model and the set of translational and rotational coordinates

This appendix details the values of the electrical elements connected to the ground obtained applying the node-voltage method from the full car model for the set of translational and rotational coordinates (see Section 3.2.2).

$$C_1 = m$$

$$C_2 = \frac{I_{G\alpha}}{W^2}$$

$$C_3 = \frac{I_{G\beta}}{L^2}$$

$$C_4 = m_{ssdi}$$

$$C_5 = m_{ssdd}$$

$$C_6 = m_{ssti}$$

$$C_7 = m_{sstd}$$

$$G_1 = \frac{\left(d_{std} - d_{sti}\right) l_t - \left(d_{sdd} + d_{sdi}\right) l_d}{L} + \frac{\left(d_{sdi} - d_{sti}\right) w_i - \left(d_{sdd} + d_{std}\right) w_d}{W}$$

$$G_2 = \frac{\left(d_{sdd} + d_{std}\right) {w_d}^2 + \left(d_{sdi} + d_{sti}\right) {w_i}^2}{W^2} + \frac{d_{sdd} l_d w_d - d_{sdi} l_d w_i - d_{std} l_t w_d + d_{sti} l_t w_i}{LW}$$

$$G_3 = \frac{\left(d_{sdd} + d_{sdi}\right) {l_d}^2 + \left(d_{std} + d_{sti}\right) {l_t}^2}{L^2} + \frac{d_{sdd} l_d w_d - d_{sdi} l_d w_i - d_{std} l_t w_d + d_{sti} l_t w_i}{LW}$$

$$G_4 = d_{rdi} + \frac{d_{sdi} l_d}{L} - \frac{d_{sdi} w_i}{W}$$

$$G_5 = d_{rdd} + \frac{d_{sdd} l_d}{L} + \frac{d_{sdd} w_d}{W}$$

$$G_6 = d_{rti} - \frac{d_{sti} l_t}{L} - \frac{d_{sti} w_i}{W}$$

$$G_7 = d_{rtd} - \frac{d_{std} l_t}{L} + \frac{d_{std} w_d}{W}$$

$$B_1 = \frac{\left(k_{std} - k_{sti}\right) l_t - \left(k_{sdd} + k_{sdi}\right) l_d}{L} + \frac{\left(k_{sdi} - k_{sti}\right) w_i - \left(k_{sdd} + k_{std}\right) w_d}{W}$$

$$B_2 = \frac{\left(k_{sdd} + k_{std}\right) {w_d}^2 + \left(k_{sdi} + k_{sti}\right) {w_i}^2}{W^2} + \frac{k_{sdd} l_d w_d - k_{sdi} l_d w_i - k_{std} l_t w_d + k_{sti} l_t w_i}{LW}$$

$$B_3 = \frac{\left(k_{sdd} + k_{sdi}\right) {l_d}^2 + \left(k_{std} + k_{sti}\right) {l_t}^2}{L^2} + \frac{k_{sdd} l_d w_d - k_{sdi} l_d w_i - k_{std} l_t w_d + k_{sti} l_t w_i}{LW}$$

$$B_4 = k_{rdi} + \frac{k_{sdi} l_d}{L} - \frac{k_{sdi} w_i}{W}$$

$$B_5 = k_{rdd} + \frac{k_{sdd} l_d}{L} + \frac{k_{sdd} w_d}{W}$$

$$B_6 = k_{rti} - \frac{k_{sti} l_t}{L} - \frac{k_{sti} w_i}{W}$$

$$B_7 = k_{rtd} - \frac{k_{std} l_t}{L} + \frac{k_{std} w_d}{W}$$

References

[1] F.A. Firestone, A new analogy between mechanical and electrical systems, J. Acoust. Soc. Am. 4 (3) (1933) 249–267.
[2] H.F. Olson, Dynamical Analogies, Van Nostrand Company, New York, NY, 1943.
[3] A. Bloch, Electromechanical analogies and their use for the analysis of mechanical and electromechanical systems, J. Inst. Electr. Eng. I Gen. 92 (52) (1945) 157–169.
[4] W.P. Mason, Electrical and mechanical analogies, Bell Syst. Tech. J. 20 (4) (1941) 405–414, http://dx.doi.org/10.1002/j.1538-7305.1941.tb03607.x.
[5] J. Miles, Applications and limitations of mechanical-electrical analogies, new and old, J. Acoust. Soc. Am. 14 (3) (1943) 183–192, http://dx.doi.org/10.1121/1.1916217.
[6] D. García-Vallejo, A. Alcayde, J. López-Martínez, F.G. Montoya, Detection of communities within the multibody system dynamics network and analysis of their relations, Symmetry 11 (12) (2019) 1525.
[7] P. Gardonio, M.J. Brennan, On the origins and development of mobility and impedance methods in structural dynamics, J. Sound Vib. 249 (3) (2002) 557–573.
[8] G. Bertuccio, On the physical origin of the electro-mechano-acoustical analogy, J. Acoust. Soc. Am. 151 (3) (2022) 2066–2076.
[9] W. Hähnle, Die Darstellung elektromechanischer Gebilde durch rein elektrische Schaltbilder, in: Wissenschaftliche Veröffentlichungen Aus Dem Siemens-Konzern, Springer, 1932, pp. 1–23.
[10] E. Jezierski, On electrical analogues of mechanical systems and their using in analysis of robot dynamics, in: Robot Motion and Control: Recent Developments, Springer, 2006, pp. 391–404.
[11] M. Akbaba, O. Dakkak, B.-S. Kim, A. Cora, S.A. Nor, Electric circuit-based modeling and analysis of the translational, rotational mechanical and electromechanical systems dynamics, IEEE Access 10 (2022) 67338–67349.
[12] E. Brandão, W.D. Fonseca, P.H. Mareze, An algorithmic approach to electroacoustical analogies, J. Acoust. Soc. Am. 152 (1) (2022) 667–678.
[13] J. Lopez-Martinez, J.C. Martinez, D. Garcia-Vallejo, A. Alcayde, F.G. Montoya, A new electromechanical analogy approach based on electrostatic coupling for vertical dynamic analysis of planar vehicle models, IEEE Access 9 (2021) 119492–119502, http://dx.doi.org/10.1109/ACCESS.2021.3108488.
[14] A. Falaize, T. Hélie, Passive modelling of the electrodynamic loudspeaker: From the thiele–small model to nonlinear port-Hamiltonian systems, Acta Acust. 4 (1) (2020) 1.
[15] N. Tiwari, A. Puri, A. Saraswat, Lumped parameter modelling and methodology for extraction of model parameters for an electrodynamic shaker, J. Low Freq. Noise Vib. Act. Control 36 (2) (2017) 99–115.
[16] D. Jeltsema, J.M.A. Scherpen, Multidomain modeling of nonlinear networks and systems, IEEE Control Syst. Mag. 29 (4) (2009) 28–59.
[17] C.W. de Silva, Modeling of Dynamic Systems with Engineering Applications, CRC Press, Boca Raton, 2017.
[18] D.C. Karnopp, D.L. Margolis, R.C. Rosenberg, System dynamics: Modeling, simulation, and control of mechatronic systems, in: EngineeringPro Collection, Wiley, 2012.
[19] A. Alabakhshizadeh, Y. Iskandarani, G. Hovland, O.M. Midtgård, Analysis, modeling and simulation of mechatronic systems using the bond graph method, Model. Identif. Control 32 (1) (2011) 35–45, http://dx.doi.org/10.4173/mic.2011.1.3.
[20] W. Marquis-Favre, E. Bideaux, O. Mechin, S. Scavarda, F. Guillemard, M. Ebalard, Mechatronic bond graph modelling of an automotive vehicle, Math. Comput. Model. Dyn. Syst. 12 (2–3) (2006) 189–202.
[21] M.J. Mashayekhi, K. Behdinan, Analytical transmissibility based transfer path analysis for multi-energy-domain systems using four-pole parameter theory, Mech. Syst. Signal Process. 95 (2017) 122–137.
[22] G.-H. Geitner, The bond graph-an excellent modelling tool to study abstraction level and structure comparison, in: 2010 IEEE Vehicle Power and Propulsion Conference, IEEE, 2010, pp. 1–7.
[23] L. Sass, J. McPhee, C. Schmitke, P. Fisette, D. Grenier, A comparison of different methods for modelling electromechanical multibody systems, Multibody Syst. Dyn. 12 (3) (2004) 209–250.
[24] L.I. Silva, G.A. Magallán, C.H. De Angelo, G.O. Garcia, Vehicle dynamics using multi-bond graphs: Four wheel electric vehicle modeling, in: 2008 34th Annual Conference of IEEE Industrial Electronics, IEEE, 2008, pp. 2846–2851.
[25] F. Pehlivan, C. Mizrak, I. Esen, Modeling and validation of 2-DOF rail vehicle model based on electro–mechanical analogy theory using theoretical and experimental methods, Eng. Technol. Appl. Sci. Res. 8 (6) (2018) 3603–3608.
[26] X. Xu, H. Jiang, M.H. Gao, Modeling and validation of air suspension with auxiliary chamber based on electromechanical analogy theory, Appl. Mech. Mater. 437 (2013) 190–193.
[27] N. Jiamei, Z. Xiaoliang, C. Long, Suspension employing inerter and optimization based on vibration isolation theory on electrical-mechanical analogies, in: 2010 International Conference on Optoelectronics and Image Processing, Vol. 2, IEEE, 2010, pp. 481–484.
[28] Y. Shen, Y. Liu, L. Chen, X. Yang, Optimal design and experimental research of vehicle suspension based on a hydraulic electric inerter, Mechatronics 61 (2019) 12–19.
[29] Y. Jiang, R. Wang, R. Ding, D. Sun, W. Liu, Design and test study of a new mixed control method for magnetorheological semi-active suspension based on electromechanical analogy theory, J. Theoret. Appl. Mech. 59 (2021).
[30] T. Zhang, X. Yang, Y. Shen, X. Liu, T. He, Performance enhancement of vehicle mechatronic inertial suspension, employing a bridge electrical network, World Electr. Veh. J. 13 (12) (2022) 229.
[31] J.Y. Routex, S. Gay-Desharnais, M. Ehsani, Study of Hybrid Electric Vehicle Drive Train Dynamics using Gyrator-Based Equivalent Circuit Modeling, Tech. Rep., SAE Technical Paper, 2002.
[32] C.M. Pappalardo, D. Guida, A time-domain system identification numerical procedure for obtaining linear dynamical models of multibody mechanical systems, Arch. Appl. Mech. 88 (2018) 1325–1347.
[33] M.M. ElMadany, A.O. Qarmoush, Dynamic analysis of a slow-active suspension system based on a full car model, J. Vib. Control 17 (1) (2011) 39–53.
[34] M.A. Abdelkareem, L. Xu, M.K.A. Ali, A. Elagouz, J. Mi, S. Guo, Y. Liu, L. Zuo, Vibration energy harvesting in automotive suspension system: A detailed review, Appl. Energy 229 (2018) 672–699.
[35] H. Xiao, X. Wang, S. John, A dimensionless analysis of a 2DOF piezoelectric vibration energy harvester, Mech. Syst. Signal Process. 58 (2015) 355–375.
[36] A. Benhiba, A. Bybi, R. Alla, D. Hilal, et al., Investigation of vibrations energy harvesting from passive car suspension using quarter car model under bump excitation, in: E3S Web of Conferences, Vol. 336, EDP Sciences, 2022, p. 00053.
[37] R. Alla, A. Bybi, A. Benhiba, H. Drissi, et al., Overview of piezoelectric energy harvesting technology in the tire condition monitoring systems, in: E3S Web of Conferences, vol. 336, EDP Sciences, 2022, p. 00022.
[38] N. Sezer, M. Koç, A comprehensive review on the state-of-the-art of piezoelectric energy harvesting, Nano Energy 80 (2021) 105567.
[39] C.R. Bowen, M.H. Arafa, Energy harvesting technologies for tire pressure monitoring systems, Adv. Energy Mater. 5 (7) (2015) 1401787.
[40] F. Qian, Y. Liao, L. Zuo, P. Jones, System-level finite element analysis of piezoelectric energy harvesters with rectified interface circuits and experimental validation, Mech. Syst. Signal Process. 151 (2021) 107440.
[41] C. Lan, Y. Liao, G. Hu, A unified equivalent circuit and impedance analysis method for galloping piezoelectric energy harvesters, Mech. Syst. Signal Process. 165 (2022) 108339.
[42] Y. Liao, J. Liang, Unified modeling, analysis and comparison of piezoelectric vibration energy harvesters, Mech. Syst. Signal Process. 123 (2019) 403–425.

[43] J. Jia, X. Shan, X. Zhang, T. Xie, Y. Yang, Equivalent circuit modeling and analysis of aerodynamic vortex-induced piezoelectric energy harvesting, Smart Mater. Struct. 31 (3) (2022) 035009.
[44] A. Abolhasani, S. Pakdelian, Comparison of control strategies and electromechanical devices for the backpack energy harvesting system, IEEE Trans. Ind. Appl. 56 (6) (2020) 6420–6435.
[45] F. Fahy, J. Walker, Advanced Applications in Acoustics, Noise and Vibration, CRC Press, 2018.
[46] D. Oshmarin, N. Sevodina, N. Iurlova, M. Iurlov, Development of an electrical analogue for modeling natural vibrations of a viscoelastic structure with piezoelectric element, J. Intell. Mater. Syst. Struct. 32 (3) (2021) 369–384.
[47] R. Darleux, B. Lossouarn, I. Giorgio, F. dell'Isola, J.-F. Deü, Electrical analogs of curved beams and application to piezoelectric network damping, Math. Mech. Solids 27 (4) (2022) 578–601.
[48] G. Raze, J. Dietrich, B. Lossouarn, G. Kerschen, Modal-based synthesis of passive electrical networks for multimodal piezoelectric damping, Mech. Syst. Signal Process. 176 (2022) 109120.
[49] L. Yuehao, C. Zhe, H. Niaoqing, Y. Yi, Y. Zhengyang, Study of dynamic breakdown of inerter and the improved design, Mech. Syst. Signal Process. 167 (2022) 108520.
[50] M.R. Bai, K.-Y. Ou, Design and implementation of electromagnetic active control actuators, J. Vib. Control 9 (8) (2003) 997–1017.
[51] F. Mamedov, R. Dadasheva, R. Guseinov, A.S. Akhmedova, N. Alieva, Mathematical model of two-step vibroexciter with low mechanical frequency, Russ. Electr. Eng. 81 (8) (2010) 447–451.
[52] Y. Qian, A. Salehian, S.-W. Han, H.-J. Kwon, Design and analysis of an ultrasonic tactile sensor using electro-mechanical analogy, Ultrasonics 105 (2020) 106129.
[53] R. Mukhiya, M. Garg, P. Gaikwad, S. Sinha, A. Singh, R. Gopal, Electrical equivalent modeling of MEMS differential capacitive accelerometer, Microelectron. J. 99 (2020) 104770.
[54] P. Luca, A. Reatti, F. Corti, R.A. Mastromauro, Inductive power transfer: Through a bondgraph analogy, an innovative modal approach, in: 2017 IEEE International Conference on Environment and Electrical Engineering and 2017 IEEE Industrial and Commercial Power Systems Europe (EEEIC/I&CPS Europe), IEEE, 2017, pp. 1–6.
[55] A. Bybi, O. Mouhat, M. Garoum, H. Drissi, S. Grondel, One-dimensional equivalent circuit for ultrasonic transducer arrays, Appl. Acoust. 156 (2019) 246–257.
[56] X. Li, P. Guo, Y. Ding, Z. Chen, X. Wang, Q. Lv, A generalized electromechanical coupled model of standing-wave linear ultrasonic motors and its nonlinear version, Mech. Syst. Signal Process. 186 (2023) 109870.
[57] C. Cuell, An electric circuit analog of a constrained mechanical system, IEEE Trans. Circuits Syst. I 48 (9) (2001) 1114–1118.
[58] M.C. Smith, Synthesis of mechanical networks: The inerter, IEEE Trans. Automat. Control 47 (10) (2002) 1648–1662.
[59] L. Chua, Memristor-the missing circuit element, IEEE Trans. Circuit Theory 18 (5) (1971) 507–519.
[60] D.B. Strukov, G.S. Snider, D.R. Stewart, R.S. Williams, The missing memristor found, Nature 453 (7191) (2008) 80–83.
[61] G.F. Oster, D.M. Auslander, The memristor: A new bond graph element, J. Dyn. Syst. Meas. Control 94 (3) (1972) 249–252, http://dx.doi.org/10.1115/1.3426595, URL arXiv:https://asmedigitalcollection.asme.org/dynamicsystems/article-pdf/94/3/249/5521411/249_1.pdf.
[62] C.W. de Silva, A systematic approach for modeling multi-physics systems, Int. J. Mech. Eng. Educ. (2019) 0306419019868801.
[63] S.S. Rao, F.F. Yap, Mechanical Vibrations, Vol. 4, Addison-Wesley New York, 1995.
[64] C.K. Alexander, M.N.O. Sadiku, M. Sadiku, Fundamentals of Electric Circuits, McGraw-Hill Higher Education Boston, 2007.
[65] T. Yuvapriya, P. Lakshmi, S. Rajendiran, Vibration suppression in full car active suspension system using fractional order sliding mode controller, J. Braz. Soc. Mech. Sci. Eng. 40 (4) (2018) http://dx.doi.org/10.1007/s40430-018-1138-0.